Friction State Classification Based on Vehicle Inertial Measurements

Donald Selmanaj, Matteo Corno and Sergio M. Savaresi

***Abstract*—Tire-road friction is the most important characteristic defining the planar dynamics of wheeled vehicles. It has consequences on the drivability, stability and tuning of the active vehicle dynamics control systems. This paper proposes two methods for the on-line estimation of the tire-road friction, with the specific goal of adapting the active vehicle dynamics control systems. The problem is framed as a classification problem where inertial measurements are used to discriminate between high and low friction regimes. The first method merges a recursive least-squares (RLS) algorithm with a heuristic bistable logic to classify the friction condition and promptly react to its changes. The second method runs a classification algorithm on the slip-acceleration bi-dimensional map. Both methods simultaneously account for the longitudinal and lateral dynamics. The methods are extensively tested on experimental data. The results show that the driving conditions play a critical role in the performance, nevertheless both methods present satisfactory results under excited conditions and detection delay can be as low as 2 sec.**

***Index Terms*—road friction, surface detection**

I. Introduction

Tire-road friction plays an essential role in the vehicle behavior. It represents the most important and the most uncertain parameter of the planar dynamics. Tire forces nonlinearly depend on a number of vehicle states (e.g. speed, sideslip angle and camber angle) and parameters (road condition, wear, etc.). These nonlinear, time-varying characteristics play a fundamental role in determining the dynamic properties of the vehicle [1], and their knowledge is especially important to model-based vehicle dynamics controllers. As the road condition changes, control systems need to guarantee robustness.

An important aspect characterizing active vehicle dynamics control systems is the tire-road friction knowledge. It distinguishes robust algorithms that do not need the tire-road friction information from algorithms that depend on the tire-road friction estimate.

In the realm of robust methods one can find methods based on the close loop control of the yaw rate. The Internal Model Control (IMC) technique is a suitable approach for designing feedback controllers that guarantee robust stability and manage the control saturation, while the combination with a feedforward action improves the transient behavior of the system, [2]. In addition to the yaw rate, the sideslip angle (i.e., the angle between the vehicle longitudinal axis and the speed vector) plays an important role in the vehicle stability. The sideslip and its derivative can be used by a supervisor to assist the yaw rate feedback controller, [3]. However, the sideslip can not be measured and need to be estimated; to this end the authors propose an estimation method unaware of the tire-road friction.

The knowledge of the tire-road friction allows for an optimized control of the available actions as it is essential for the knowledge of the tire force limits. In [4], the authors propose a two-level control scheme. The first level, composed by a nonlinear sliding mode controller, determines the generalized tire forces required to achieve the vehicle motion objectives. The second level distributes the effort on each wheel and takes into account for the tire-road friction. The estimation of the latter is used in emergency braking maneuvers in automated highway systems, [5]; the authors exploit the friction knowledge to determine the pressure in the master cylinder of the braking system and achieve maximum deceleration during braking. Other studies focus on over-actuated vehicles (i.e., four-wheel steering and driving vehicles) and present control schemes that employ the friction estimation to maximize the forces exerted by the tires on the road [6]. The wide use of friction information in control systems is the reason for the effort dedicated to its estimate.

One characteristic classifying the friction estimation methods is the sensor layout. Three layouts can be found in the literature: inertial, combined GPS (Global Positioning System) and inertial, and "Smart-tire". Their main differences regard the sensors reliability and costs.

"Smart-tire" systems refer to tires equipped with sensors for monitoring the tire thermal and mechanical parameters during driving [7]. "In-tire" accelerometers are also a possible choice [8]. "Smart-tire" applicability to commercial vehicles is still limited and researchers have focused their efforts in developing methods that exploit the vehicle dynamics and rely on vehicle measurements. Measurement layouts using GPS, [9], [10], or combination of GPS with brake and motor torque measurements as well as inertial measurements, [11], can improve the estimation of the vehicle state and, as a consequence, the estimation of the tire friction. However, GPS presents issues in terms of reliability, as the measurements are not always available and methods relying only on inertial measurements are preferred. The present work is focused on low-cost off-the-shelf senors, common in consumer vehicles. The measurement layout includes vehicle inertial quantities (i.e., vehicle accelerations and angular rates), wheels angular speeds and steering wheel angle.

Estimation methods based on inertial measurements can be classified in three main groups: (i) methods exploiting the longitudinal vehicle dynamics, (ii) methods exploiting the lateral dynamics and (iii) methods exploiting both dynamics.

Longitudinal dynamic based methods exploit the relation

D. Selmanaj, M. Corno and S. M. Savaresi are with the Dipartimento di Elettronica, Informazione e Bioingegneria, Politecnico di Milano, Piazza L. da Vinci, 32, 20133, Milano, Italy.

between the longitudinal slip and the longitudinal tire force, which converts to vehicle acceleration. The friction characteristic is estimated by analyzing the longitudinal stiffness or the maximum longitudinal force. Based on this relation a Kalman Filter (KF) observer can be designed for each driving wheel, [12], and a fault detection algorithm is integrated to manage the fast variations of the friction. The main weaknesses of the approach are the limited driving conditions that do not include braking and the requirement of the traction force. A method extended to braking conditions is presented in [13]. The method uses the relation between the longitudinal stiffness and the maximum friction force while still requiring the estimate of the traction force and the normal load. In [12], [13] the estimation quality of the friction is indeed affected by the accuracy of longitudinal forces estimation. To improve the estimate of the longitudinal force, in [14], the authors enhance the traction force observer with normal force, brake pressure and tire radii observers. Although the method shows promising results its main drawback is the dependency of traction force estimation from the engine map; the latter is highly dependent on the running conditions and is not robust for online estimation algorithms. To overcome the dependency on the traction force alternative studies rely on the brake pressure measuerement, see e.g. [15], [16]. Although simulation, [15], and experimental, [16], results show the effectiveness of the methods, the applied brake pressure is not always available.
The main drawback of methods relying only on the longitudinal dynamics is their functioning range, limited to braking and accelerating maneuvers. They do not work if the vehicle is performing nearly constant speed curves.

Lateral dynamic based methods employ the relation between the lateral forces generated by the tires and the lateral slips. The lateral forces are obtained through the vehicle single-track model and the inertial measurements while the tire lateral slips are obtained as algebraic functions of the vehicle state. Depending on the available inertial measurements the cornering stiffness can be estimated by means of the lateral dynamics, yaw dynamics or a combination of the two, [17]. Based on the relation between the vehicle lateral dynamics and the tire-road friction, in [18], the authors propose a loop approach for estimating the cornering stiffnesses from the tire lateral slips, the tire maximum forces making use of the cornering stiffnesses and the tire lateral slips by using the maximum tire forces. The method results are shown on short experimental maneuvers and the paper lacks a sensitivity analysis of the slip observer to the estimated friction. Other approaches are based on the well known Extended Kalman Filter (EKF). By describing the vehicle dynamics with the single-track model and augmenting the state with the front and rear cornering stiffnesses, in [19], the authors show promising results on simulation data. The same approach is exploited in [20], where the capabilities of the EKF are shown in short experimental tests. EKF is suitable for different model representations of the vehicle and the tires. A combination of the vehicle single-track model and the tire Burckhard/Kiencke model is employed in [21]. The authors use a nonlinear adaptive model of the tire and show that designing an EKF on the adaptive model is advantageous compared to non adaptive linear and nonlinear models. The main weakness of the EKF based approaches is the analysis of the system observability. The studies focus on short dynamic maneuvers and lack the analysis of the methods behavior on unexcited maneuvers. The excitation of the driving conditions is a physical boundary that limits the estimation capabilities of all the methods; if the driving conditions are not excited the influence of the tire-road friction on the vehicle behavior is undetectable. Estimation methods based only on the lateral or longitudinal dynamics are limited respectively to turning conditions or accelerating/braking maneuvers. With the goal of expanding the driving conditions of the estimation methods, different studies exploit both dynamics.

EKF is suitable also for combined dynamics. In [22], the authors design an EKF to estimate the vehicle state and the tire forces (longitudinal and lateral); the friction is estimated as the rate between the friction forces and the nominal vertical loads. The method presents satisfactory results on low sideslip angle experimental tests, but lacks the analysis of the unexcited conditions and the convergence time. A different approach exploiting longitudinal and lateral dynamics is proosed in [23]. The authors distinguish four conditions: (1) during lateral medium excitation conditions a closed loop nonlinear observer estimates the vehicle state and the friction; (2) during lateral high excitation conditions the estimation employs the self-aligning torque of the front wheels and requires the steering torque measurement; (3) during longitudinal small excitation condition the longitudinal stiffness is estimated through RLS and (4) during longitudinal high excitation conditions the RLS algorithm is employed to estimate the friction peak. To integrate the four methods an algorithm employing combined slip Brush model and a four-wheel vehicle model is proposed. The method presents promising results on a long experimental test, however the interaction between the vehicle state estimation and the friction estimation is the weakest point of the approach. Indeed, during low sideslip angle maneuvers the friction estimate presents not justified abrupt changes. Besides methods using closed loop observers (EKF) or recursive methods (RLS) a diagnostic-based approach is presented in [24]. The estimations of the instantaneous longitudinal friction and lateral forces are obtained by algebraic computations of the vehicle single-track model. These quantities are then used as inputs for the friction predictor, build on the Dugoff model. The method is tested only on short maneuvers and it is not clear if the maneuvers include curves.

For all approaches, the estimation of the tire-road friction presents two main challenges, the estimation of the vehicle state and the excitation of the running conditions. To the extent of the authors knowledge these aspects are not considered in previous approaches. This paper is focused on the distinction of two extreme conditions: high friction and low friction. For this purpose two methods are proposed. The first method employs a modified RLS algorithm, which estimates the friction based on the vehicle measurements during excited condition and uses external information during unexcited conditions. The second method is based on a nonlinear classification approach and estimates the friction by opportunely weighting the slip-acceleration maps of the vehicle. Both methods focus on the

fast detection of the friction change.
The paper is organized as follows. In Section II, the vehicle and tire modeling are described. Section III introduces a modified version of the RLS algorithm, which here is referred as bistable RLS (*bRLS*), and demonstrates the algorithm functioning on artificial data. The first method, which employs the bRLS algorithm, is presented in Section IV while the second method is presented in V. Section VI shows the results obtained on experimental data. The paper ends with some concluding remarks in Section VII.

II. Vehicle model

The methods presented in this work exploit the vehicle inertial measurements and the vehicle single-track model relating the tire-road friction with the vehicle measurements. Figure 1 shows the model and the quantities involved. The equations

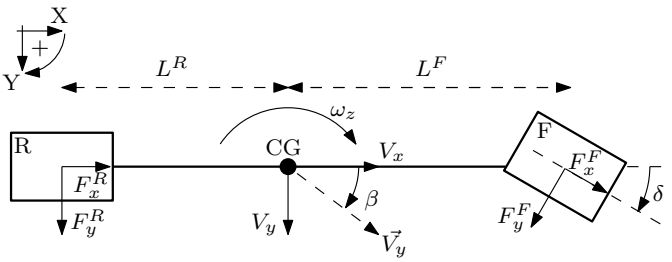

Figure 1. Vehicle single-track model.

modeling the longitudinal and the lateral dynamics can be approximated for small steering angles (δ) as follows:

$$\begin{aligned} Ma_x &= \cos\delta \cdot F_x^F + F_x^R \approx F_x^F + F_x^R \\ Ma_y &= \cos\delta \cdot F_y^F + F_y^R \approx F_y^F + F_y^R \\ I_z\dot{\omega}_z &= L^F \cos\delta \cdot F_y^F - L^R F_y^R \approx L^R F_y^F - L^R F_y^R, \end{aligned} \tag{1}$$

where a_x and a_y are the vehicle longitudinal and lateral accelerations, ω_z is the yaw rate, M is the vehicle mass and I_z is the moment of inertia. F_x^F and F_x^R are the longitudinal forces exerted by the front and the rear tires respectively, F_y^F and F_y^R are the lateral forces exerted by the front and the rear tires respectively. The development of a complete vehicle model requires the definition of the tire force model and researchers have dedicated a considerable effort to this end.

The tire forces depend mainly on the tire slips; the longitudinal slip is the difference between the vehicle and the tire longitudinal speed and the lateral slip is the tire sideslip angle (i.e., the angle between the tire longitudinal axis and the tire speed vector). For small slips, tires present a linear behavior, and the forces are determined by the longitudinal stiffness $\left(C_k = \frac{\partial F_x}{\partial k}\big|_{k=0}\right)$ and cornering stiffnesses $\left(C_\alpha = \frac{\partial F_y}{\partial \alpha}\Big|_{\alpha=0}\right)$. However, as the slips increase, the tire forces saturate and present a complex behavior, Figure 2. The tire-road friction limits the maximum forces exerted by tires, the dynamical behavior as well the drivability limits of the vehicle. Due to the complexity of the phenomena and the unknown factors, such as road surface, models for different use have been developed. In [25], the authors present an overview of the existing models. Complex models can precisely describe the behavior of the tire, however they require ad-hoc experiments for the estimation of the unknown parameters. For online estimation problems researchers have focused their efforts on simple models which are easy to combine with the vehicle model.

This combination requires the definition of the tire slips. The longitudinal slip can be computed by the following expression:

$$k^i = \frac{r \cdot \omega^i - V_x}{\max\left(V_x, r \cdot \omega^i\right)}, \quad i = FL, FR, RL, RR, \tag{2}$$

where ω and r are the wheel speed and radius respectively and V_x is the vehicle longitudinal speed.
The tire lateral slips depend on the vehicle state according to the following relations:

$$\begin{aligned} \alpha^F &= \arctan\left(\frac{V_y^F}{V_x^F}\right) \approx \beta - \delta + \omega_z \frac{L^F}{V_x} \\ \alpha^R &= \arctan\left(\frac{V_y^R}{V_x^R}\right) \approx \beta - \omega_z \frac{L^R}{V_x} \end{aligned}, \tag{3}$$

where V_x^F, V_x^R are the longitudinal velocities of the tires, V_y^F, V_y^R are their lateral velocities and L^F, L^R are the distances of axles from the vehicle center of mass. As Equation (3) shows the tire lateral slips can be approximated as linear expressions of the vehicle state.

The computation of the tire slips requires the yaw rate (ω_z), the steering wheel angle (δ), the wheel rotational speeds (ω), the vehicle longitudinal speed (V_x) and the sideslip angle (β). While ω_z, δ and ω can be measured by reliable sensors, V_x and β need to be estimated. In this paper, V_x and β are estimated with the methods presented in [26]. The estimation methods rely on kinematic approaches and do not require the knowledge of the tire-road friction; this decouples the estimation of the tire-road friction from the estimation of the vehicle state.

The paper is focused on the fast detection of the friction condition rather than the exact determination of the its characteristic. To this purpose, if similar front and real axle stiffnesses are considered, the following linear equations are derived by (1), (2) and (3):

$$\begin{aligned} a_x &= \frac{C_k}{M}\left(k^{FL} + k^{FR} + k^{RL} + k^{RR}\right) \\ a_y &= \frac{2C_\alpha}{M}\left(\alpha^F \cos\delta + \alpha^R\right). \end{aligned} \tag{4}$$

Therefore, the behavior of the vehicle resembles the behavior of an equivalent tire, relating the vehicle longitudinal acceleration with the sum of the wheel longitudinal slips and the vehicle lateral acceleration with the sum of the wheel lateral slips. Figure 2 depicts some experimental data collected on high and low friction roads and a nonlinear model of the tire (opportunely scaled). The good fit of the two is the main motivation of the methods proposed in this paper. The two friction conditions can be distinguished by focusing on the linear relation of the measurements, i.e. the slopes of the accelerations at nearly zero slip or the nonlinear relation, i.e. the maximum acceelerations reached at high slips.

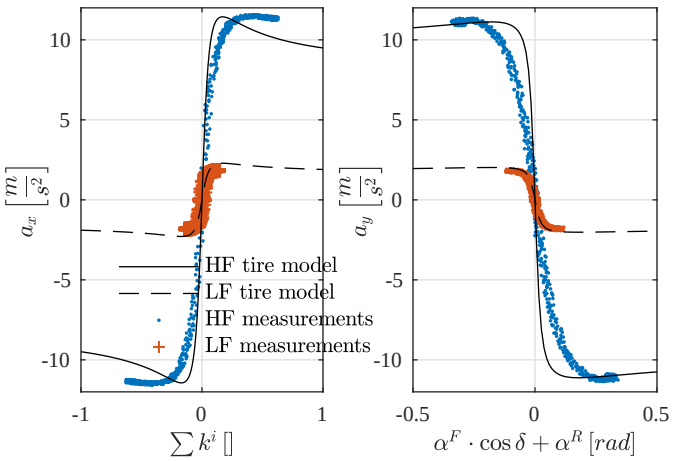

Figure 2. Low friction (LF) and high friction (HF) data distribution on the slip-acceleration planes.

III. RLS WITH REFERENCE

In the realm of Prediction Error Methods (PEM), the recursive least-square (RLS) is a well known algorithm for identifying unknown parameters in linear regression models. Given the following linear regression model:

$$y(t) = \varphi(t)^T \theta(t), \tag{5}$$

y is referred as the model output, φ is referred as the regressor and θ is the unknown parameter vector to be estimated.
With regard to the problem of the tire stiffness estimation and the quantities involved in the vehicle linear model, (4), $\theta_k = \frac{C_k}{M}$ and $\theta_\alpha = \frac{2C_\alpha}{M}$ are the parameters to be estimated, $y_k = a_x$ and $y_\alpha = a_y$ are the outputs of the two linear regressions, $\varphi_k = k^{FL} + k^{FR} + k^{RL} + k^{RR}$ and $\varphi_\alpha = \alpha^F \cos\delta + \alpha^R$ are the two regressors.
The RLS provides a reliable solution for the on-line estimation of the unknown parameter vector with proven convergence properties under the assumption of persistent excitation [27], [28].

The RLS algorithm presents two main drawbacks that need addressing:

- The lack of *persistent excitation* limits the estimation capabilities. For the problem at hand the lack of persistent excitation corresponds to soft acceleration, braking and turning maneuvers. During these conditions the behavior of the parameters estimated through the RLS presents abrupt variations and can diverge;
- The algorithm does not provide the possibility of merging the data with *external information*. The present work is focused on the fast discrimination between low and high friction. For both conditions a priori values of the corresponding longitudinal and lateral stiffnesses can be computed offline. These information can be used online to accelerate the estimation of the friction.

Here an addition to the RLS algorithm is proposed and the modified algorithm is referred as *bRLS*. It is capable of managing the unexcited conditions and includes the a priori external information in the estimation process. The modification regards the prediction error computation as shown by the following equations:

$$\begin{aligned}
\hat{\theta}(t) &= \hat{\theta}(t-1) + K(t)\,\boldsymbol{\varepsilon^{ref}(t)} \\
K(t) &= S(t)\,\varphi(t) \\
\varepsilon(t) &= y(t) - \varphi(t)^T \hat{\theta}(t-1) \\
\boldsymbol{\varepsilon^{ref}(t)} &= \left(\mathbf{1} - \boldsymbol{e^{-\gamma|\varphi(t)|}}\right)\boldsymbol{\varepsilon(t)} \\
&\quad + \boldsymbol{e^{-\gamma|\varphi(t)|}\varphi(t)^T}\left(\boldsymbol{\theta^{ref}(t)} - \boldsymbol{\hat{\theta}(t-1)}\right) \\
S(t) &= \frac{S(t-1) - \eta(t-1)^{-1} S(t-1)\,\varphi(t)\varphi(t)^T S(t-1)}{\mu} \\
\eta(t-1) &= \mu + \varphi(t)^T S(t-1)\,\varphi(t),
\end{aligned} \tag{6}$$

where μ is the forgetting factor and determines the convergence speed and the accuracy of the estimate. High values of μ lead to slower and smoother estimates.

During unexcited conditions, when $|\varphi|$ is small, the prediction error is modified in order to drive the estimate to a reference (θ^{ref}). The estimate reference represents a preferred value for the parameters to be estimated or values given by an external mechanism. In Section III-A a method to turn off the estimate if the data are not excited is introduced, while in Section III-B the *bRLS* is combined with a state machine for fast classification of the parameter. The parameter γ needs tuning and determines the φ-region where the estimate is driven to the reference. Figure 3 shows the weight of the data compared to the weight of the reference for a range of the regressor; as φ decreases, the influence of the new data on the estimate is decreased.

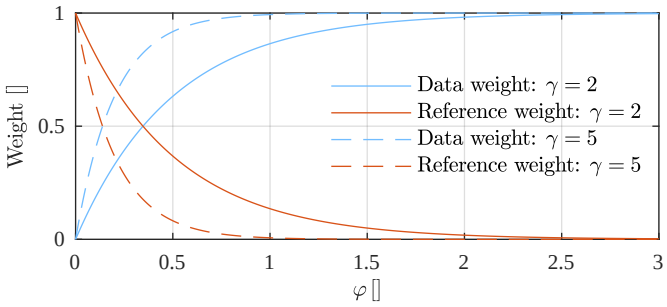

Figure 3. *bRLS* measurement VS reference weighting.

A. Smooth estimation turn off with the bRLS

The *bRLS* algorithm can be used to manage conditions with unexcited data. By imposing

$$\theta^{ref} = \hat{\theta}(t-1), \tag{7}$$

the estimate is driven to its previous values when φ is small. This is equivalent to smoothly turning off the algorithm and in the extreme case φ=0 the estimate preserves its old value. Figure 4 shows the results obtained on artificial data with μ=0.96. The results of the RLS are compared with the *bRLS* for three different values of γ. As γ decreases the behavior of the *bRLS* tends to the behavior of the RLS algorithm. The modified algorithm allows the use of small values of the

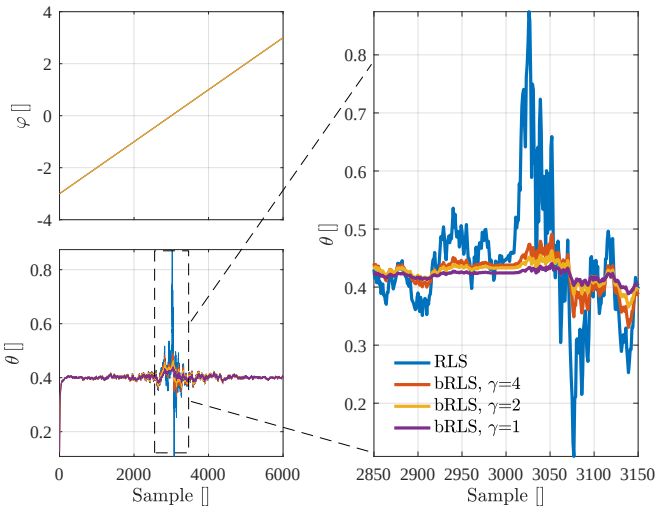

Figure 4. Smooth turn off of RLS estimation algorithm (μ=0.96).

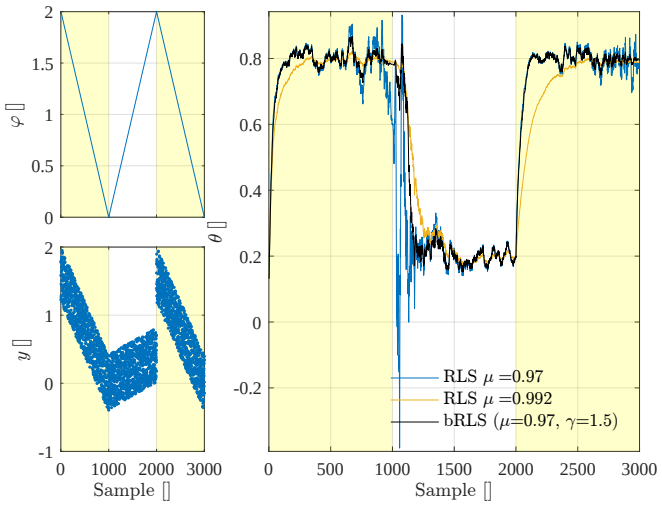

Figure 6. Parameter classification with *bRLS* on artificial data.

forgetting factor (μ) for a fast convergence time and avoids abrupt changes in the estimation during unexcited conditions.

B. Fast classification with the bRLS

One possibility for using the *bRLS* to classify parameter clusters or ranges is shown in Figure 5. A state machine keeps trace of the current state of the parameter and provides to the *bRLS* algorithm the appropriate reference of the parameter. For each state the parameter reference can be obtained by a priori knowledge of the problem at hand. Regarding the friction condition estimation, extensive tests on known high friction and low friction road can provide the parameter reference for each state. The state machine manages the switch between the parameter states. Here a threshold condition is used. The

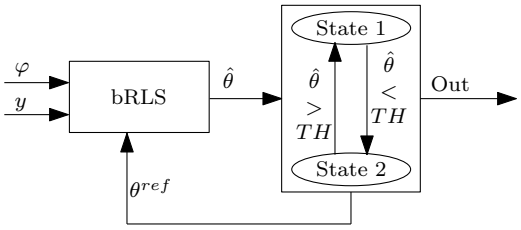

Figure 5. Schematic of the *bRLS* algorithm used for fast classification.

forgetting factor of the *bRLS* can be set to low values in order to have fast convergence of the estimate during excited conditions, while γ determines the behavior for unexcited conditions. Figure 6 shows the results obtained on artificial data with noise. The parameter presents two transitions: (i) step transition from 0.8 to 0.2 at sample=1000; (ii) step transition from 0.2 to 0.8 at sample=2000. The estimation is initialized at $\hat{\theta}(0)$=0.2 and $S(0)$=100. The estimate presents two transitions at excited conditions (i.e., initial and at sample=2000). During these transitions the method behaves as a fast RLS and converges quickly to the new parameter value. During the unexcited transition (sample=1000) the reference influences the estimate behavior and the method behaves as a slow RLS. The state machine transition is managed by the comparison with a threshold. To obtain the results of Figure 6, the threshold is 0.6.

IV. Grip estimate through bRLS

The method of Figure 5 can be adapted to the problem of friction classification as shown in Figure 7. Two instances of the *bRLS* algorithm run in parallel; one instance estimates the longitudinal stiffness and one estimates the cornering stiffness. One state machine keeps trace of the friction state and manages its transitions.

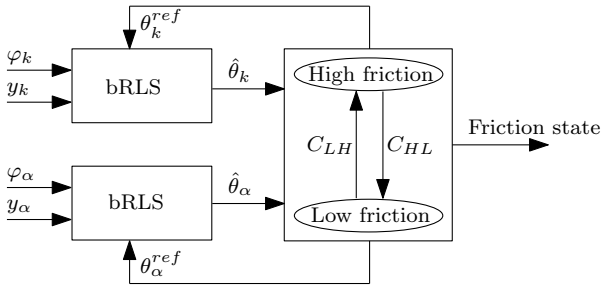

Figure 7. *bRLS* algorithm applied to road friction identification.

The transitions are activated by the followings conditions:

$$\begin{aligned} C_{LH} &= \hat{\theta}_\alpha < \theta_\alpha^{threshold} \ \text{ OR } \ \hat{\theta}_k > \theta_k^{threshold} \\ C_{HL} &= \hat{\theta}_\alpha > \theta_\alpha^{threshold} \ \text{ OR } \ \hat{\theta}_k < \theta_k^{threshold} \end{aligned} \tag{8}$$

Therefore, the estimated friction state can change if sufficiently excited data are measured on the longitudinal or the lateral dynamics.

V. Nonlinear Classification

The *bRLS* algorithm estimates the friction condition through the longitudinal and the lateral stiffness. The slip-force planes of the vehicle are separated by a line (i.e., thresholds on the longitudinal and lateral stiffness) and the two regions define the two friction conditions. The method proposed in this Section separates the low and high friction regions considering

for the nonlinearities of the tire-road interaction and employs the distribution of the data on the slip-acceleration planes, Figure 2. Three main regions can be identified on these planes. The low slip low acceleration region corresponds to low excitation running conditions; both friction conditions present measurements in this region and these data are not reliable for the distinction of the friction condition. The large slip low acceleration region is typical of low friction roads and the large acceleration condition is typical of high friction roads.
The low slip and acceleration regions are identified by comparison with thresholds while the high and low friction regions can be distinguished using the tire medium friction curve. Therefore, given the slip estimates, references of the longitudinal (a_x^{ref}) and lateral (a_y^{ref}) accelerations can be computed. If $|a_x| > \left|a_x^{ref}\right|$, or $|a_y| > \left|a_y^{ref}\right|$ the current state of the friction is high, otherwise it is low. The reference curves are computed by the Pacejka tire model, [29]. The two characteristics are assumed to be independent: the longitudinal reference curve is computed with zero lateral slip and the lateral reference curve is computed with zero longitudinal slip.
The distribution of the samples with respect to the reference curve indicates the state of the friction, while the distance of a sample from the reference curve indicates the reliability of the measure. A sample close to the reference curve is at the border of the two friction conditions (i.e., can be caused by both conditions) and is less reliable compared to samples that are distant from the reference curve. Based on this reasoning, to each sample a weight expressing the reliability of the sample is assigned; $\left|a_x - a_x^{ref}\right|$ determines the reliability of the longitudinal dynamics data and $\left|a_y - a_y^{ref}\right|$ determines the reliability of the lateral dynamics data. The weighting of the samples is computed by the following exponential equation:

$$W_i = 1 - e^{-\frac{\left(a_i - a_i^{ref}\right)^2}{\sigma_i^2}}, \quad i = x, y, \tag{9}$$

where σ_i are two design parameters. Here, $\sigma_x = 3$ and $\sigma_y = 2$ are used.
Merging the exponential weighting and the nonlinear tire characteristics, Figure 8 and 9 are obtained. They express the reliability weight assigned to samples on the slip-acceleration planes. In addition to the exponential weighting the low slip low acceleration regions are not considered as they are shared by the two friction conditions. The second and fourth quadrant of the longitudinal dynamics and the first and third quadrant of the lateral dynamics are not considered as data in these quadrants are caused by measurement noise and estimate errors and do not represent the real behavior of the vehicle.
Based on the weighting maps of Figure 8 and 9 three probability indexes are computed:

- p^H is the probability that the current samples correspond to high friction. It is computed as the average of p_k^H and p_α^H, given by:

$$p_k^H = \begin{cases} W_x & \text{if } |a_x| > \left|a_x^{ref}\right| \\ 0 & \text{if } |a_x| < \left|a_x^{ref}\right| \end{cases}, \tag{10}$$

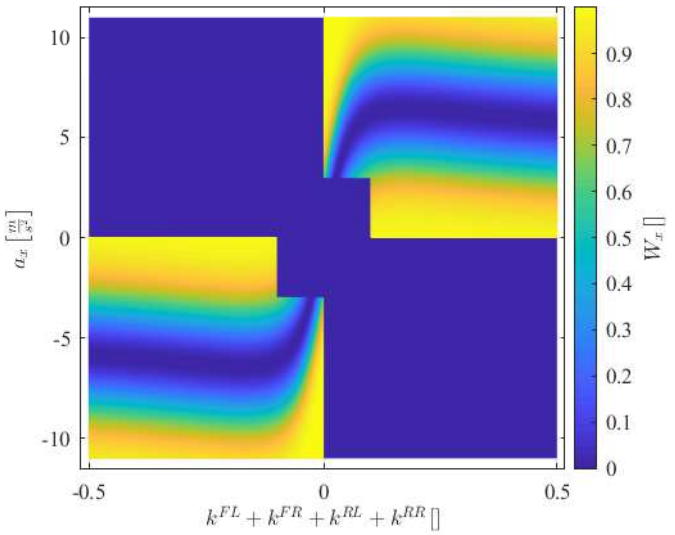

Figure 8. Nonlinear weighting of longitudinal dynamics.

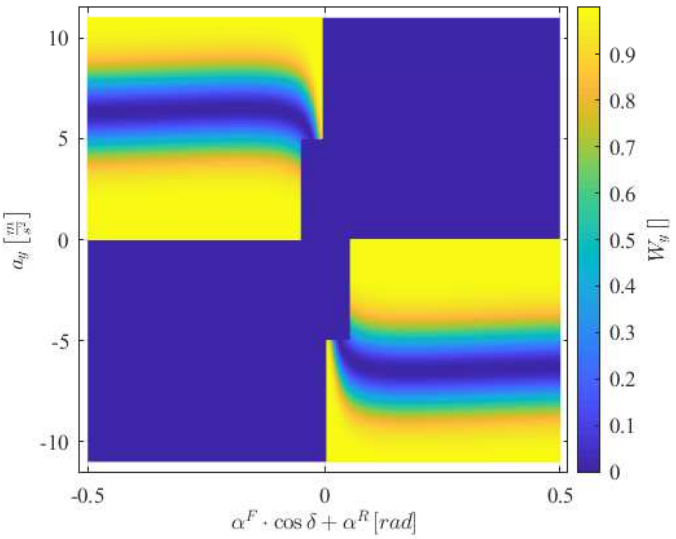

Figure 9. Nonlinear weighting of lateral dynamics.

$$p_\alpha^H = \begin{cases} W_y & \text{if } |a_y| > \left|a_y^{ref}\right| \\ 0 & \text{if } |a_y| < \left|a_y^{ref}\right| \end{cases}, \tag{11}$$

- p^L is the probability that the current samples correspond to low friction. It is computed as the average of p_k^L and p_α^L, given by:

$$p_k^L = \begin{cases} W_x & \text{if } |a_x| < \left|a_x^{ref}\right| \\ 0 & \text{if } |a_x| > \left|a_x^{ref}\right| \end{cases}, \tag{12}$$

$$p_\alpha^L = \begin{cases} W_y & \text{if } |a_y| < \left|a_y^{ref}\right| \\ 0 & \text{if } |a_y| > \left|a_y^{ref}\right| \end{cases}, \tag{13}$$

- p^O is the probability that the friction condition is equal to its previous state. It is computed as the average of p_k^O and p_α^O, given by:

$$p_k^O = 1 - W_x \tag{14}$$

$$p_\alpha^O = 1 - W_y \tag{15}$$

Given p^O, p^L and p^H the friction condition is estimated by:

$$\hat{F} = p^O \cdot \hat{F}\,(k-1) + p^H \cdot v^H + p^L \cdot v^L, \qquad (16)$$

where v^H and v^L represent desired output values for the high and low friction conditions. Here $v^H = 1$ and $v^L = 0$ are chosen. The complete method is shown in Figure 10. It includes a low-pass filter that determines the convergence speed of the method and is chosen based on the measurement noise.

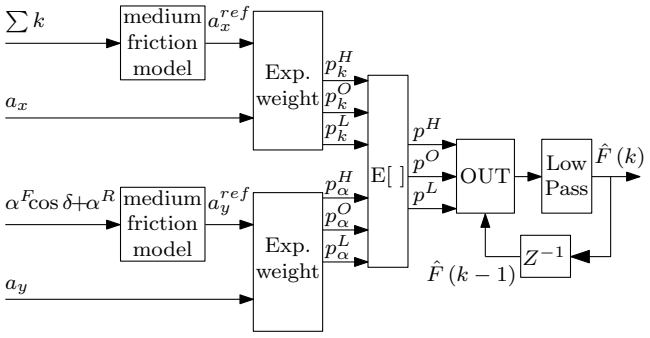

Figure 10. Nonlinear classification scheme.

VI. Experimental results

The method presented in previous Sections are tested and compared on experimental data. For all the trials the vehicle is equipped with a 6DOF inertial measurement unit (IMU), wheels speed measurements, steer angle measurement and an optical system providing the longitudinal speed and the sideslip angle measurement.

The test is composed of three parts. During the first and the third part the vehicle runs on a dry asphalt track (i.e., high friction) and during the second part the vehicle runs on a gravel track (i.e., low friction). Figure 11 present the results of the longitudinal speed and sideslip angle estimation obtained with the kinematic method presented in [26], which does not require the friction knowledge. During the high friction track the vehicle runs at higher speed while on the gravel track it presents higher sideslip angles. The estimates present higher error during the gravel surface, as during this track the measurements have higher noise levels. These estimates are used as inputs in the methods proposed here.

A. Results with the bRLS method

The *bRLS* method detects the friction state and its changes by estimating the longitudinal and lateral stiffness. The estimate is smoothly turned off as the excitation of the data vanishes, i.e. $\varphi \approx 0$. This behavior is evident in Figure 12 at 185 s <t< 250 s. Although the road condition changes from high to low friction at t=184 s, the method reacts at t=234.4 s as the corresponding maneuver (starting at t=233.8 s) is the first sufficiently excited during the low friction road. A second drawback of using a linear method to weight informative data (i.e. $\varphi > 0$) is shown at t=341 s when the driver is performing a strong acceleration. Although y_k reaches high values, this maneuver is not considered in the estimation of the new state because φ_k is in the range of not excitation.

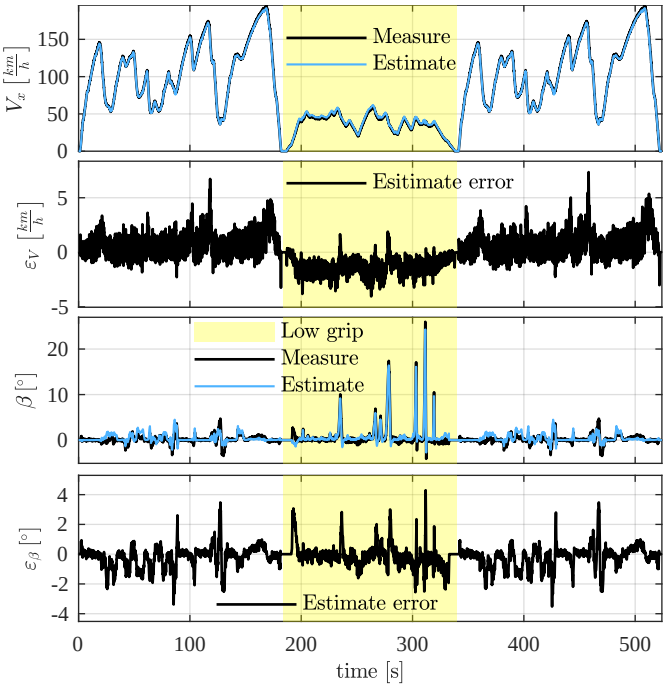

Figure 11. Vehicle longitudinal speed estimate.

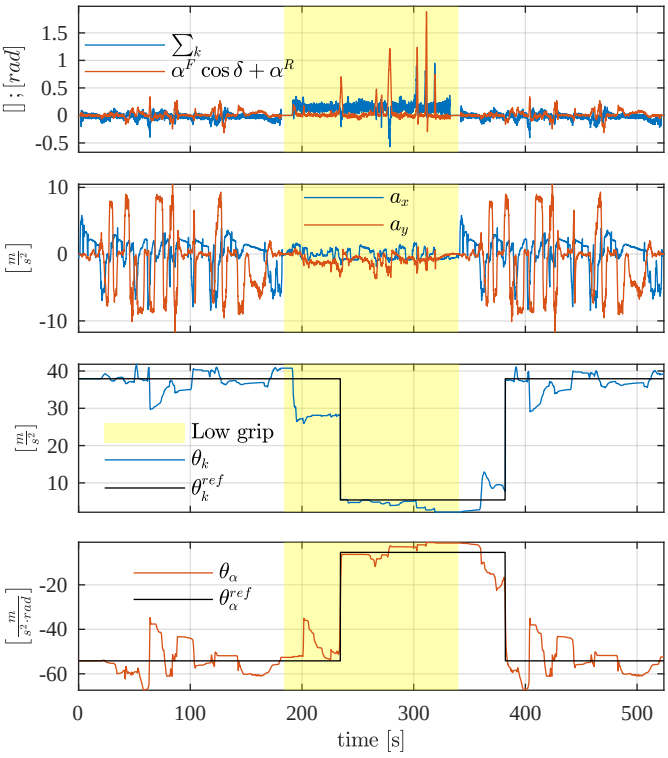

Figure 12. *bRLS* results.

B. Results with the nonlinear method

The reference curve and the regions used by the nonlinear classification method to split the slip-acceleration planes fit the nonlinear behavior of the pneumatic, hence the vehicle. This translates in a higher accuracy which allows the detection of the friction change with low excitation maneuver. This behavior can be seen in Figure 13 at t=191 s with the first maneuver in the switch from high to low friction road.

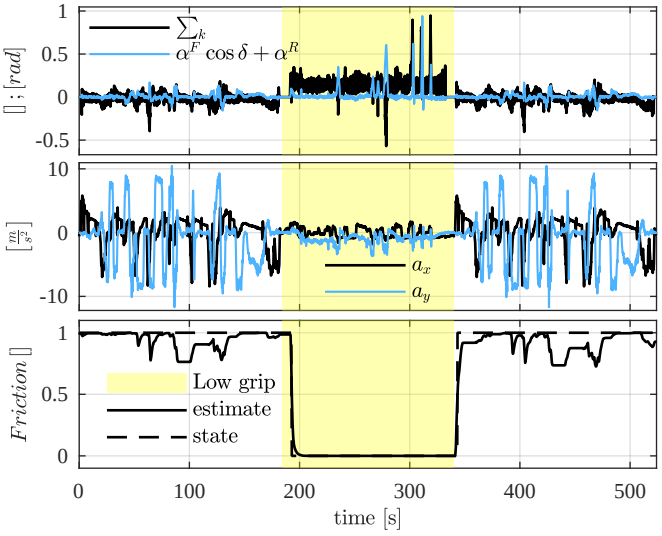

Figure 13. Nonlinear classification results.

C. Comparison of the methods

VII. Conclusion

The estimation of the road friction is crucial for chassis control problems; it determines the vehicle handling limits and dynamical behavior. A considerable difficulty with the road friction regards the knowledge of the exact characteristic, which is time varying and is a nonlinear function of the tire slips. The methods proposed in this paper are focused on the fast classification of the friction condition, distinguishing between high and low friction.

References

[1] U. Kiencke and L. Nielsen, *Automotive Control Systems For Engine, Driveline, and Vehicle*, 2nd ed. Springer-Verlag Berlin Heidelberg, 2005.

[2] M. Canale, L. Fagiano, M. Milanese, and P. Borodani, "Robust vehicle yaw control using an active differential and {IMC} techniques," *Control Engineering Practice*, vol. 15, no. 8, pp. 923–941, 2007.

[3] G. Panzani, M. Corno, M. Tanelli, A. Zappavigna, S. M. Savaresi, A. Fortina, and S. Campo, "Designing on-demand four-wheel-drive vehicles via active control of the central transfer case," *Intelligent Transportation Systems, IEEE Transactions on*, vol. 11, no. 4, pp. 931–941, Dec 2010.

[4] J. Wang and R. G. Longoria, "Coordinated vehicle dynamics control with control distribution," in *American Control Conference, 2006*. IEEE, June 2006, pp. 5348–5353.

[5] J. Yi, L. Alvarez, and R. Horowitz, "Adaptive emergency braking control with underestimation of friction coefficient," *Control Systems Technology, IEEE Transactions on*, vol. 10, no. 3, pp. 381–392, 2002.

[6] E. Ono, Y. Hattori, Y. Muragishi, and K. Koibuchi, "Vehicle dynamics integrated control for four-wheel-distributed steering and four-wheel-distributed traction/braking systems," *Vehicle System Dynamics*, vol. 44, no. 2, pp. 139–151, 2006.

[7] A. Pohl, R. Steindl, and L. Reindl, "The "intelligent tire" utilizing passive saw sensors measurement of tire friction," *Instrumentation and Measurement, IEEE Transactions on*, vol. 48, no. 6, pp. 1041–1046, 1999.

[8] S. M. Savaresi, M. Tanelli, P. Langthaler, and L. D. Re, "New regressors for the direct identification of tire deformation in road vehicles via "in–tire" accelerometers," *Control Systems Technology, IEEE Transactions on*, vol. 16, no. 4, pp. 769–780, 2008.

[9] D. M. Bevly, J. Ryu, and J. C. Gerdes, "Integrating ins sensors with gps measurements for continuous estimation of vehicle sideslip, roll, and tire cornering stiffness," *Intelligent Transportation Systems, IEEE Transactions on*, vol. 7, no. 4, pp. 483–493, 2006.

[10] J.-O. Hahn, R. Rajamani, and L. Alexander, "Gps-based real-time identification of tire-road friction coefficient," *Control Systems Technology, IEEE Transactions on*, vol. 10, no. 3, pp. 331–343, 2002.

[11] R. Rajamani, G. Phanomchoeng, D. Piyabongkarn, and J. Y. Lew, "Algorithms for real-time estimation of individual wheel tire-road friction coefficients," *Mechatronics, IEEE/ASME Transactions on*, vol. 17, no. 6, pp. 1183–1195, 2012.

[12] F. Gustafsson, "Slip-based tire-road friction estimation," *Automatica*, vol. 33, no. 6, pp. 1087–1099, 1997.

[13] S. Muller, M. Uchanski, and K. Hedrick, "Estimation of the maximum tire-road friction coefficient," *Journal of dynamic systems, measurement, and control*, vol. 125, no. 4, pp. 607–617, 2003.

[14] C. Lee, K. Hedrick, and K. Yi, "Real-time slip-based estimation of maximum tire-road friction coefficient," *Mechatronics, Ieee/Asme Transactions On*, vol. 9, no. 2, pp. 454–458, 2004.

[15] N. Patel, C. Edwards, and S. K. Spurgeon, "A sliding mode observer for tyre friction estimation during braking," in *American Control Conference, 2006*. IEEE, 2006, pp. 6–pp.

[16] M. Tanelli, L. Piroddi, and S. M. Savaresi, "Real-time identification of tire–road friction conditions," *IET control theory & applications*, vol. 3, no. 7, pp. 891–906, 2009.

[17] C. Sierra, E. Tseng, A. Jain, and H. Peng, "Cornering stiffness estimation based on vehicle lateral dynamics," *Vehicle System Dynamics*, vol. 44, no. sup1, pp. 24–38, 2006.

[18] L. Haffner, M. Kozek, J. Shi, and H. P. Jörgl, "Estimation of the maximum friction coefficient for a passenger vehicle using the instantaneous cornering stiffness," in *American Control Conference, 2008*. IEEE, 2008, pp. 4591–4596.

[19] M. C. Best, T. Gordon, and P. Dixon, "An extended adaptive kalman filter for real-time state estimation of vehicle handling dynamics," *Vehicle System Dynamics*, vol. 34, no. 1, pp. 57–75, 2000.

[20] P. Bolzern, F. Cheli, G. Falciola, and F. Resta, "Estimation of the Non-Linear Suspension Tyre Cornering Forces from Experimental Road Test Data," *Vehicle System Dynamics*, vol. 31, no. 1, pp. 23–34, 1999. [Online]. Available: http://www.tandfonline.com/doi/abs/10.1076/vesd.31.1.23.2100

[21] G. Baffet, A. Charara, and G. Dherbomez, "An observer of tire–road forces and friction for active security vehicle systems," *Mechatronics, IEEE/ASME Transactions on*, vol. 12, no. 6, pp. 651–661, 2007.

[22] J. Dakhlallah, S. Glaser, S. Mammar, and Y. Sebsadji, "Tire-road forces estimation using extended kalman filter and sideslip angle evaluation," in *American Control Conference, 2008*. IEEE, 2008, pp. 4597–4602.

[23] C. Ahn, H. Peng, and H. E. Tseng, "Robust estimation of road friction coefficient using lateral and longitudinal vehicle dynamics," *Vehicle System Dynamics*, vol. 50, no. 6, pp. 961–985, 2012.

[24] J. Villagra, B. D'Andréa-Novel, M. Fliess, and H. Mounier, "A diagnosis-based approach for tire–road forces and maximum friction estimation," *Control engineering practice*, vol. 19, no. 2, pp. 174–184, 2011.

[25] A. Porcel, P. Laurence, M. Basset, and G. Gissinger, "Tyre model for vehicle simulation: overview and real time solution for critical situations," in *Control Applications, 2001.(CCA'01). Proceedings of the 2001 IEEE International Conference on*. IEEE, 2001, pp. 817–822.

[26] D. Selmanaj, M. Corno, G. Panzani, and S. M. Savaresi, "Vehicle sideslip estimation: A kinematic based approach," *Control Engineering Practice*, vol. 67, pp. 1 – 12, 2017.

[27] L. Ljung and T. Söderström, *Theory and Practice of Recursive Identification*, ser. The MIT Press Series in Signal Processing, Optimization, and Control, 1983, no. 4.

[28] S. Bittanti, P. Bolzern, and M. Campi, "Recursive least-squares identification algorithms with incomplete excitation: convergence analysis and application to adaptive control," *Automatic Control, IEEE Transactions on*, vol. 35, no. 12, pp. 1371–1373, 1990.

[29] E. Bakker, L. Nyborg, and H. B. Pacejka, "Tyre modelling for use in vehicle dynamics studies," SAE Technical Paper, Tech. Rep., 1987.